State-Variable Analysis of Wireless Power Transfer Networks for Linear and Nonlinear Loads

David M. Beams, Anusha Papasani
Department of Electrical Engineering
University of Texas at Tyler
Tyler, TX 75799 USA
dbeams@uttyler.edu

***Abstract*— A state-equation approach to modeling wireless power transfer (WPT) networks is presented. The state-variable approach was investigated because it permits termination of the network in nonlinear loads, which is not possible with the usual analysis with the phasor transform. The modeling work presented here involves a three-coil WPT network terminated in a rectifier and filter; simulation has been carried out using constant-resistance and constant-power loads. The validity of the model was established by comparison with commercial circuit-analysis software.**

Keywords- wireless power transfer, nonlinear loads ,state variables

I. INTRODUCTION

The concept of transmission of electric power by wireless power transfer (WPT) was presented by Nicola Tesla over a century ago. In recent years there have appeared numerous papers analyzing WPT systems with linear loads, e.g. [1]. However, the principal approach utilized in this work has been sinusoidal steady-state analysis using the phasor transform. The phasor transform is limited to analysis of linear, time-invariant networks. Most WPT network applications, however, end in delivery of power to a dc load and require a rectifier and filter; in addition, switching-type dc-to-dc converters present constant-power loads. A state-equation approach, however, allows analysis of such nonlinear systems. This paper presents development and validation of a preliminary simplified state-variable model of a WPT network with nonlinear loads.

II. SYSTEM TOPOLOGY

A. Basic four-coil WPT system

Figure 1 below shows a basic four-coil WPT system. The source side of the WPT system is comprised of voltage source V_{sq} (with associated output resistance R_s), inductors L_1 and L_2, and capacitors C_1 and C_2. The load side consists of inductors L_3 and L_4, capacitor C_3, and load resistor R_L. Linked fluxes produce mutual inductances M_{12}, M_{13}, M_{14}, M_{23}, and M_{34}. The equivalent series resistances (ESRs) of the inductors are represented by R_1–R_4. This topology is proposed in [2] and analyzed in greater detail in [3]; [4] presents a similar topology that employs symmetric input and load sides (omitting C_1).

Sinusoidal, steady-state analysis by means of the phasor transform may be applied to the circuit of Fig. 1 by decomposing the square-wave source V_{sq} into its harmonic components. For this type of analysis, V_{sq} is replaced by a sinusoidal source v_s at the appropriate frequency. High Q in the resonators L_2/C_2 and L_3/C_3 ensures that only the fundamental component of the square-wave driving voltage produces significant delivery of energy.

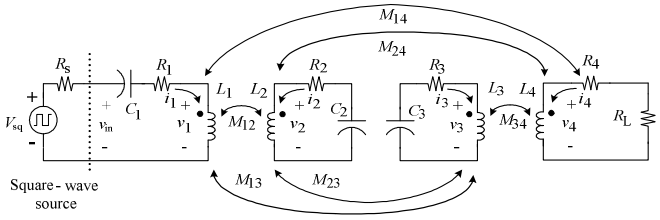

Fig.1. Basic four-coil WPT system including loss elements and resistive load.

Analysis of this network is straightforward if the appropriate component and parametric values are known *a priori*. However, design is a much-more complex task [5].

B. Modified four-coil WPT system with full-wave bridge rectifier output

A modified four-coil WPT system with full-wave bridge rectifier is shown in Fig 2 below.

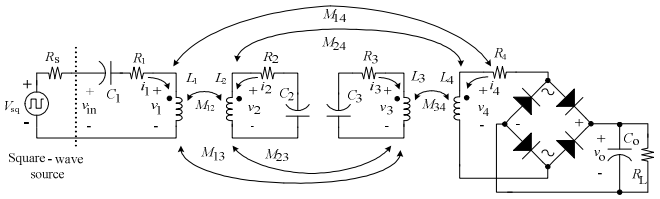

Fig.2. Modified four-coil WPT system with full-wave bridge rectifier

It is identical to the four-coil WPT system of Fig. 1 except that a full-wave bridge rectifier and storage capacitor C_o have

been added between the load resistance output coil L_4 and load resistor R_L.

C. *Three-coil WPT system with full- wave bridge rectifier output*

A simplified model of modified four-coil WPT system with a full-wave bridge rectifier is shown in Fig. 3. This is a 3-coil model that includes only the direct (principal) mutual inductances to make problem tractable. Here, L_1 is removed and the open-circuit induction into L_2 by i_1 is represented by a voltage source $v_S = \omega M_{12}|\, i_1|$ in series with L_2. Given that the spacing of L_1 - L_3 and L_1 - L_4 are relatively large, their mutual inductances were neglected in the simplified model proposed in Fig. 3. Similarly, mutual inductance M_{24} was omitted due to the large separtion between L_2 and L_4. This is similar to other analyses that also make this assumption [6].

As a result of current steering occurring in the full-wave bridge rectifier, the following cases must be considered in deriving the state equations for the network of Fig. 3: $i_4 < 0$, $i_4 > 0$, and $i_4 = 0$. The case $i_4 = 0$ must further be subdivided into cases based on whether the open-circuit induction into L_4 from i_3 ($= \omega M_{34}|\, i_3|$) would be sufficient to forward-bias diodes in the bridge rectifier or not. Diodes in the bridge rectifier have been represented as ideal devices in the derivations that follow.

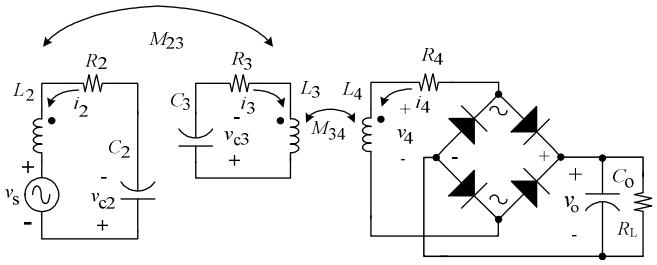

Fig.3. Three-coil WPT system with full-wave bridge rectifier output

For the case $i_4 < 0$:

$$\frac{di_2}{dt} = -\frac{i_2 R_2}{L_2} - \frac{v_{c2}}{L_2} - \frac{M_{23}}{L_2}\frac{di_3}{dt} - \frac{v_s}{L_2} \tag{1}$$

$$\frac{di_3}{dt} = -\frac{i_3 R_3}{L_3} - \frac{v_{c3}}{L_3} - \frac{M_{23}}{L_3}\frac{di_2}{dt} - \frac{M_{34}}{L_3}\frac{di_4}{dt} \tag{2}$$

$$\frac{di_4}{dt} = -\frac{M_{34}}{L_4}\frac{di_3}{dt} - \frac{i_4 R_4}{L_4} + \frac{v_o}{L_4} \tag{3}$$

$$\frac{dv_{c2}}{dt} = \frac{i_2}{C_2} \tag{4}$$

$$\frac{dv_{c3}}{dt} = \frac{i_3}{C_3} \tag{5}$$

$$\frac{dv_o}{dt} = -\frac{i_4}{C_o} - \frac{v_o}{C_o R_L} \tag{6}$$

Substituting (1) and (3) into (2) allows a state equation for di_3/dt to be derived in terms of state variables and input source voltage v_s. This expression may then be substituted into (1) and (3) to derive state equations for the other two inductor currents i_2 and i_4. After this process, the state equations for the inductor current are:

$$\begin{aligned}\frac{di_2}{dt} = \left(\frac{1}{1-{k_{23}}^2-{k_{34}}^2}\right)\Bigg\{ &-\left[\frac{R_2\left(1-{k_{23}}^2-{k_{34}}^2\right)}{L_2} + \frac{{M_{23}}^2}{{L_2}^2 L_3}R_2\right] i_2 + \frac{M_{23}}{L_2}\frac{R_3}{L_3} i_3 - \frac{M_{34}M_{23}}{L_2 L_3 L_4} R_4 i_4 \\ &- \left[\frac{\left(1-{k_{23}}^2-{k_{34}}^2\right)}{L_2} + \frac{{M_{23}}^2}{{L_2}^2 L_3}\right] v_{c2} \\ &+ \frac{M_{23}}{L_2 L_3} v_{c3} + \frac{M_{34}M_{23}}{L_2 L_3 L_4} v_o \\ &- \left[\frac{\left(1-{k_{23}}^2-{k_{34}}^2\right)}{L_2} + \frac{{M_{23}}^2}{{L_2}^2 L_3}\right] v_s \Bigg\}\end{aligned} \tag{7}$$

$$\begin{aligned}\frac{di_3}{dt} = \left(\frac{1}{1-{k_{23}}^2-{k_{34}}^2}\right)\Bigg\{ &\frac{M_{23}}{L_2 L_3} R_2 i_2 - \frac{R_3}{L_3} i_3 + \frac{M_{34}}{L_4 L_3} R_4 i_4 \\ &+ \frac{M_{23}}{L_2 L_3} v_{c2} - \frac{1}{L_3} v_{c3} - \frac{M_{34}}{L_4 L_3} v_o + \frac{M_{23}}{L_2 L_3} v_s \Bigg\}\end{aligned} \tag{8}$$

$$\begin{aligned}\frac{di_4}{dt} = \left(\frac{1}{1-{k_{23}}^2-{k_{34}}^2}\right)\Bigg\{ &-\frac{M_{34}M_{23}}{L_2 L_3 L_4} R_2 i_2 + \frac{M_{34}}{L_4 L_3} R_3 i_3 \\ &- \left[\frac{R_4\left(1-{k_{23}}^2-{k_{34}}^2\right)}{L_4} + \frac{{M_{34}}^2}{{L_4}^2 L_3} R_4\right] i_4 \\ &- \frac{M_{34}M_{23}}{L_2 L_3 L_4} v_{c2} + \frac{M_{34}}{L_4 L_3} v_{c3} \\ &+ \left[\frac{\left(1-{k_{23}}^2-{k_{34}}^2\right)}{L_4} + \frac{{M_{34}}^2}{{L_4}^2 L_3}\right] v_o \\ &- \frac{M_{34}M_{23}}{L_2 L_3 L_4} v_s \Bigg\}\end{aligned} \tag{9}$$

where k_{23} is the flux-coupling coefficient of inductors L_2 and L_3 and k_{34} is the flux-coupling coefficient of inductors L_3 and L_4.

For the case $i_4 > 0$, differential equations (3) and (6) are altered:

$$\frac{di_4}{dt} = -\frac{M_{34}}{L_4}\frac{di_3}{dt} - \frac{i_4 R_4}{L_4} - \frac{v_o}{L_4} \tag{10}$$

$$\frac{dv_o}{dt} = \frac{i_4}{C_o} - \frac{v_o}{C_o R_L} \tag{11}$$

After the appropriate substitutions, the state equations for the inductor currents for the case $i_4 > 0$ become:

$$\frac{di_2}{dt}=\left(\frac{1}{1-{k_{23}}^2-{k_{34}}^2}\right)\Bigg\{-\Bigg[\frac{R_2\left(1-{k_{23}}^2-{k_{34}}^2\right)}{L_2}+\frac{{M_{23}}^2}{{L_2}^2L_3}R_2\Bigg]i_2+\frac{M_{23}}{L_2}\frac{R_3}{L_3}i_3-\frac{M_{34}M_{23}}{L_2L_3L_4}R_4i_4-\Bigg[\frac{\left(1-{k_{23}}^2-{k_{34}}^2\right)}{L_2}+\frac{{M_{23}}^2}{{L_2}^2L_3}\Bigg]v_{c2}+\frac{M_{23}}{L_2L_3}v_{c3}-\frac{M_{34}M_{23}}{L_2L_3L_4}v_o-\Bigg[\frac{\left(1-{k_{23}}^2-{k_{34}}^2\right)}{L_2}+\frac{{M_{23}}^2}{{L_2}^2L_3}\Bigg]v_s\Bigg\} \tag{12}$$

$$\frac{di_3}{dt}=\left(\frac{1}{1-{k_{23}}^2-{k_{34}}^2}\right)\Big\{\frac{M_{23}R_2}{L_2L_3}i_2-\frac{R_3}{L_3}i_3+\frac{M_{34}R_4}{L_4L_3}i_4+\frac{M_{23}}{L_2L_3}v_{c2}-\frac{1}{L_3}v_{c3}+\frac{M_{34}}{L_4L_3}v_o+\frac{M_{23}}{L_2L_3}v_s\Big\} \tag{13}$$

$$\frac{di_4}{dt}=\left(\frac{1}{1-{k_{23}}^2-{k_{34}}^2}\right)\Bigg\{-\frac{M_{34}M_{23}}{L_2L_3L_4}R_2i_2+\frac{M_{34}}{L_4L_3}R_3i_3-\Bigg[\frac{R_4\left(1-{k_{23}}^2-{k_{34}}^2\right)}{L_4}+\frac{{M_{34}}^2}{{L_4}^2L_3}R_4\Bigg]i_4-\frac{M_{34}M_{23}}{L_2L_3L_4}v_{c2}+\frac{M_{34}}{L_4L_3}v_{c3}-\Bigg[\frac{\left(1-{k_{23}}^2-{k_{34}}^2\right)}{L_4}+\frac{{M_{34}}^2}{{L_4}^2L_3}\Bigg]v_o-\frac{M_{34}M_{23}}{L_2L_3L_4}v_s\Bigg\} \tag{14}$$

If $i_4 = 0$, the bridge rectifier will conduct if the magnitude of the open-circuit induction $M_{34} \mid di_3/dt \mid > v_o$. In the case that $i_4 = 0$ and $M_{34} \cdot di_3/dt > v_o$, diodes of the bridge rectifier will permit conduction in the same way as if $i_4 < 0$. In this case, (4)–(9) remain valid. If $i_4 = 0$ and $M_{34} \cdot di_3/dt < -v_o$, the bridge rectifier will permit conduction in the same way as if $i_4 > 0$, and (4), (5), and (11)–(14) apply.

If $i_4 = 0$ and $M_{34} \mid di_3/dt \mid < v_o$, the full-wave bridge rectifier will not conduct and the differential equations of the system become:

$$\frac{di_3}{dt}=\left(\frac{1}{1-{k_{23}}^2}\right)\Big\{\frac{M_{23}}{L_2L_3}R_2i_2-\frac{R_3i_3}{L_3}+\frac{M_{23}}{L_2L_3}v_{c2}-\frac{v_{c3}}{L_3}+\frac{M_{23}}{L_2L_3}v_s\Big\} \tag{15}$$

$$\frac{di_2}{dt}=\left(\frac{1}{1-{k_{23}}^2}\right)\Bigg\{-i_2\Bigg[\frac{R_2\left(1-{k_{23}}^2\right)}{L_2}+\frac{{M_{23}}^2}{{L_2}^2L_3}R_2\Bigg]+\frac{M_{23}}{L_2}\frac{R_3}{L_3}i_3-v_{c2}\Bigg[\frac{\left(1-{k_{23}}^2\right)}{L_2}+\frac{{M_{23}}^2}{{L_2}^2L_3}\Bigg]+\frac{M_{23}}{L_2L_3}v_{c3}-v_s\Bigg[\frac{\left(1-{k_{23}}^2\right)}{L_2}+\frac{{M_{23}}^2}{{L_2}^2L_3}\Bigg]\Bigg\} \tag{16}$$

$$\frac{dv_o}{dt}=-\frac{v_o}{C_oR_L} \tag{17}$$

$$\frac{di_4}{dt}=0 \tag{18}$$

III. Simulation Methods and Results

A. Simulation methods

The state equations outlined above were programmed as a Matlab function. The following representative values were assigned to each variable:

$L_2 = 35.24\mu H$; $C_2 = 71.88nF$; $R_2 = 0.086\Omega$; $L_3 = 33.3\mu H$; $C_3 = 71.88nF$; $R_3 = 0.086\Omega$; $L_4 = 11.91\mu H$; $R_4 = 0.042\Omega$; $k_{23} = 0.1$; $k_{34} = 0.2$; $C_o = 250\mu F$.

The open-circuit induction in L_2 (v_s) was a $20V_{peak}$ sinusoid at 100kHz. Solutions to the differential equations were computed with the Matlab ode45 numerical-integration function.

B. Comparison of state-variable simulation of three-coil network with circuit-simulation software

Simulations were conducted with the three-coil network terminated in a resistive load $R_L = 5\Omega$. Figure 4 below shows the coil currents for the three-coil WPT system after sufficient time has elapsed for steady-state conditions to have been achieved.

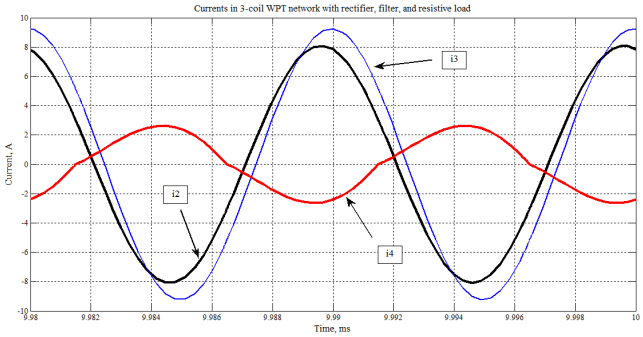

Fig.4. Coil currents i_2, i_3, and i_4 for the three-coil WPT system with bridge rectifier, filter, and resistive load. The load resistance was 5Ω and load power was approximately 13W.

Figure 5 shows the same currents computed with Multisim (National Instruments, Austin, TX). The rectifier was

implemented with four SS26 Schottky-barrier rectifiers. Comparison of Figs. 4 and 5 shows evident agreement.

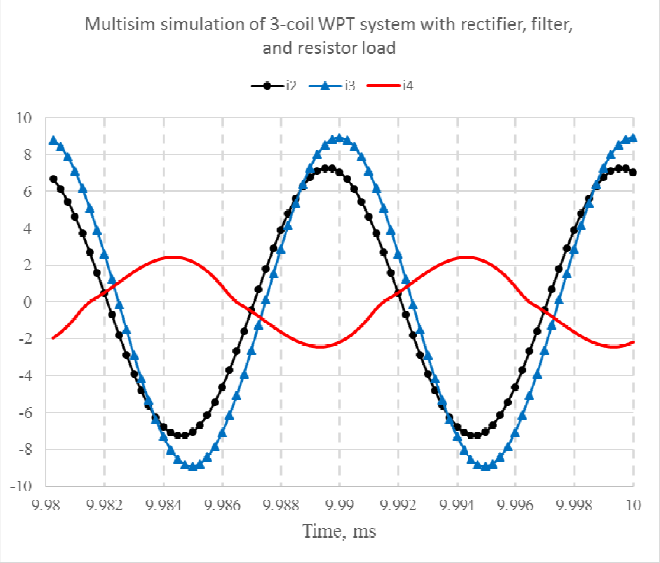

Fig.5. Coil currents i_2, i_3, and i_4 for the three-coil WPT system with bridge rectifier, filter, and 5Ω resistive load computed by Multisim.

Simulations were also carried out with load resistances of 2.5Ω and10Ω. The distortion in the waveform of i_4 became more evident for increased load resistance values. However, the waveforms i_2 and i_3 remain sinusoidal even when i_4 was highly distorted.

C. State-variable simulation of three-coil network with rectifier and constant-power load

Fig. 6 shows the coil currents and Fig. 7 shows the output voltage for a three-coil WPT system with a 10W constant-power dc load. The load was assumed to be a dc-to-dc buck converter with a +5V output. The dc-to-dc converter was assumed to be an open circuit until a minimum of +8.0V was attained at the buck converter input. Simulations were also performed for constant-power loads of 5W, 20W, and 50W.

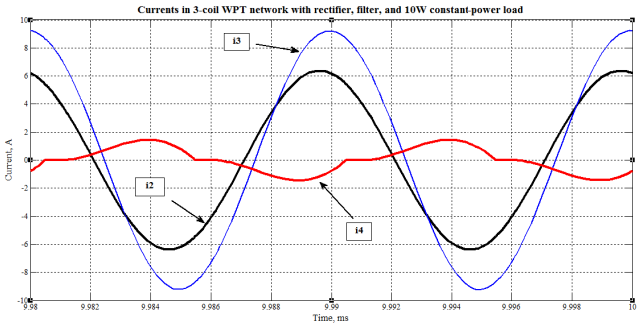

Fig.6. Currents i_2, i_3, and i_4 for three-coil WPT system with bridge rectifier, filter, and 10W constant-power load. The sinusoidal nature of currents i_2 and i_3 is evident despite the highly-distorted load current i_4.

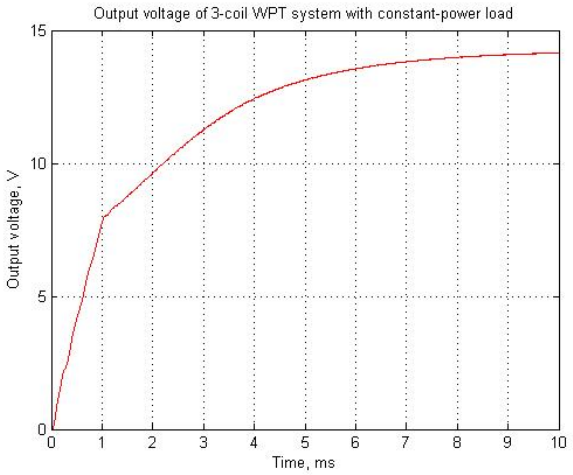

Fig. 7. Filter capacitor voltage vs. time for the three-coil WPT network with bridge rectifier and 10W constant-power load. The load was assumed to begin drawing power once the filter capacitor voltage reached 8.0V.

IV. CONCLUSIONS

A state-equation model for a three-coil WPT network with nonlinear loads has been simulated. The solutions obtained by simulation of the state-variable model have been compared to a verified model of a WPT network with a resistive load. Further extension of the model to a four-coil topology is being undertaken, as well as more-realistic modeling of nonlinear loads.

REFERENCES

[1] S.Y.R. Hui, W.X. Zhong and C.K. Lee, "A Critical Review of Recent Progress in Mid-Range Wireless Power Transfer," *IEEE Transaction on power electronics,* Vol.pp.

[2] Chih-Jung Chen, Tah-Hsiung Chu, Chih-Lung Lin, and Zeui-Chown Jou. "A Study of Loosely Coupled Coils for Wireless Power Transfer." *IEEE Transactions on Circuits and Systems–II: Express Briefs*, Vol. 57, No. 7 (July, 2010), pp. 546-540.

[3] Cannon,B., Hoburg, J., Stancil, D., and Goldstein,S. "Magnetic Resonant Coupling As a Potential Means for Wireless Power Transfer to Multiple Small Receivers." *IEEE Transactions on Power Electronics,* Vol. 24, No. 7 (July, 2009), pp. 1819-1825.

[4] Cheon, S.; Kim, Y-H.; Kang, S-Y; Lee, M.; Lee, J-M.; and Zyung, T. "Circuit-Model-Based Analysis of a Wireless Energy-Transfer System via Coupled Magnetic Rosances." *IEEE Transactions on Industrial Electronics,* Vol. 58, No. 7 (July, 2011), pp. 2906-2914.

[5] David M.Beams, and Sravan G. Annam. "Validation of a Reflected-Impedance Design Method for Wireless Power Transfer Applications." Proceedings of 2012 International Midwest Symposium on Circuits and system (MWSCAS), Aug 5-8, 2012, pp. 758-761.

[6] Mehdi Kiani, Uei-Ming Jow *and* Maysam Ghovanloo, "Design and Optimization of a 3-Coil Inductive Link for Efficient Wireless Power Transmission," *IEEE transactions on Biomedical Circuits and Systems*,Vol. 5,No. 6 (Dec, 2011), pp. 579-591.